Dalton
www.rsc.org/dalton

Hydrogenase on an electrode: a remarkable heterogeneous catalyst †

Sophie E. Lamle,[a] Kylie A. Vincent,[a] Louise M. Halliwell,[a] Simon P. J. Albracht[b] and Fraser A. Armstrong*[a]

[a] *Inorganic Chemistry Laboratory, Oxford University, South Parks Road, Oxford, UK OX1 3QR. E-mail: fraser.armstrong@chem.ox.ac.uk*

[b] *Swammerdam Institute for Life Sciences, Biochemistry, University of Amsterdam, Plantage Muidergracht 12, NL-1018 TV Amsterdam, The Netherlands*

Received 2nd June 2003, Accepted 30th June 2003
First published as an Advance Article on the web 22nd September 2003

Hydrogenases – enzymes interconverting hydrogen and water – display intriguing chemistry and offer important possibilities for future energy technologies. The so-called [NiFe]-hydrogenases contain a binuclear NiFe catalytic center coordinated by thiolates, CO and CN^-. Hydrogenases pose significant experimental challenges due to O_2-sensitivity, high activity, and the presence of many different active and inactive states. However, the enzyme can be studied with considerable precision using a minuscule quantity adsorbed on an electrode. In this form it is a heterogeneous catalyst rather than the solution system studied by enzymologists: in particular, exploitation of the 'potential dimension' enables complex reactions to be analysed and deconvoluted.

Introduction

Immobilised enzymes are important biotechnological agents with large practical advantages, although as with other types of heterogeneous catalysts, it is difficult to determine mechanisms and detect intermediates.[1,2] Electrochemistry provides an important and distinct example of heterogeneous catalysis, as the catalyst is usually immobilised on the electrode that provides the source or sink for electrons.[3] As we advocate in this paper, the electrocatalyst can be an enzyme, such as [NiFe]-hydrogenase, that displays remarkably high activity.[4–11] Because it is 'wired' to an electrode, the catalyst and its activity can be controlled very effectively: the potential can be varied over a wide and continuous range to drive reactions in different directions; there is excellent temporal resolution (for example the potential can be modulated, or stepped 'instantaneously' from one value to another to initiate or terminate a reaction); the flux of small solution species can be controlled (the electrode can be rotated at high speed to draw in substrate or disperse the product); then, furthermore, the rate of catalysis (turnover) is determined *directly* as current. With a redox enzyme we achieve a combination that can provide both fundamental insight and technological opportunities. The cartoon in Fig. 1 depicts molecules of hydrogenase, adsorbed in an electroactive manner at a rotating disc electrode, confronted with different substrates and inhibitors.

Hydrogenases catalyse interconversion between H_2 and protons (water) in a diverse range of microorganisms.[12–14] With little exception they are metalloenzymes, in which the active sites comprise either two Fe atoms (the all-Fe hydrogenases) or Ni and Fe ([NiFe]-hydrogenases). In either case the active sites are buried, and special channels and pathways must exist for the transfer of H_2 and H^+ to and from the solvent, while electrons are conveyed to and from the natural redox partners by one or more Fe–S clusters. The binuclear centres in each case are unusual, as aside from having several thiolate–metal bonds, they contain CO and CN^- ligands; consequently, they have a closer resemblance to organometallic catalysts than any other enzyme active site identified so far.[15–21] The inset to Fig. 1 depicts the framework of the [NiFe] centre that is expected to prevail during catalysis, *i.e.* the Ni and the Fe are bridged by

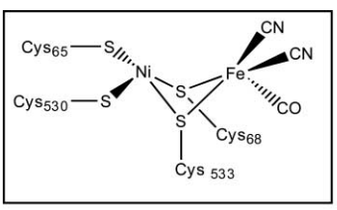

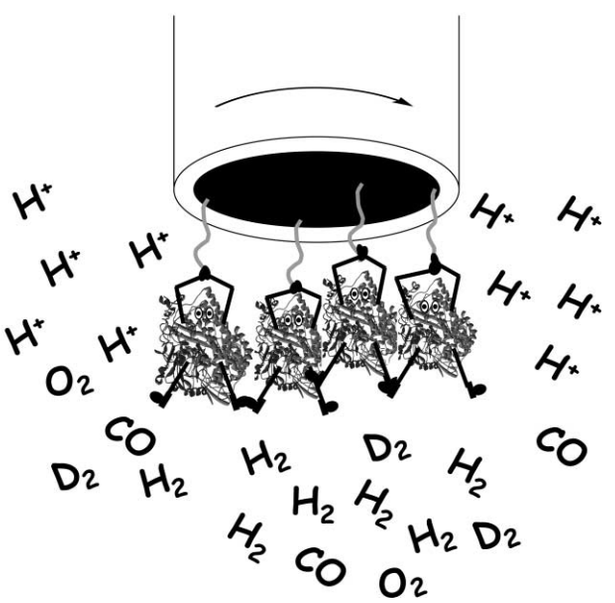

Fig. 1 Cartoon depicting [NiFe]-hydrogenase molecules adsorbed at a rotating pyrolytic graphite 'edge' (PGE) electrode and interacting with small molecules.

two cysteine thiolates, but lack the bridging O-ligand that is coordinated in the oxidised inactive forms (see below). The all-Fe hydrogenases are very active in the direction of proton reduction; whereas with [NiFe]-hydrogenases, proton reduction is subject to product inhibition and they operate most effectively in the direction of H_2 oxidation. Unlike H_2/H^+ interconversion at a Pt catalyst, which occurs by a homolytic mechanism involving H-atoms, the enzymes use a heterolytic mechanism involving separation and combination of H^+ and H^- (hydride).[22–28]

† Based on the presentation given at Dalton Discussion No. 6, 9–11th September 2003, University of York, UK.

DOI: 10.1039/b306234c

Like Pt, the [NiFe]-hydrogenase from the purple bacterium *Allochromatium vinosum* is a remarkably active electrocatalyst. This follows from studies in which hydrogenase is adsorbed on a pyrolytic graphite 'edge' (PGE) electrode, for which we estimated, conservatively, that the turnover number k_{cat} easily exceeds 1500 s^{-1} at 30 °C and probably lies closer to 10^4 s^{-1} at 45 °C (see Appendix).[6,7] The X-ray structure of the closely related hydrogenase from *Desulfovibrio gigas* shows that there are two subunits with a total molecular mass of about 90 kDa: the buried [NiFe] active site that is located in subunit A is 'wired' to the protein surface by a series of three Fe–S clusters ([4Fe–4S], [3Fe–4S] and [4Fe–4S]) located in subunit B.[16–18]

Hydrogenase exists in a number of different states which are depicted in Scheme 1. These have been studied by EPR, EXAFS, FTIR and X-ray crystallography.[14–21,29,30] Interestingly, it is the Ni entity that is redox-active, while as far as can be ascertained, the Fe remains throughout as low-spin Fe(II). The active enzyme can be oxidised to either of two inactive Ni(III) forms, called 'ready' and 'unready'. The 'ready' form is activated within minutes under H_2 at ambient temperature, whereas 'unready' requires much longer periods of incubation. It is not clear exactly how 'ready' and 'unready' differ in structure, but both are believed to contain an O-donor ligand that forms an additional bridge between the Ni and the Fe.[31–35]

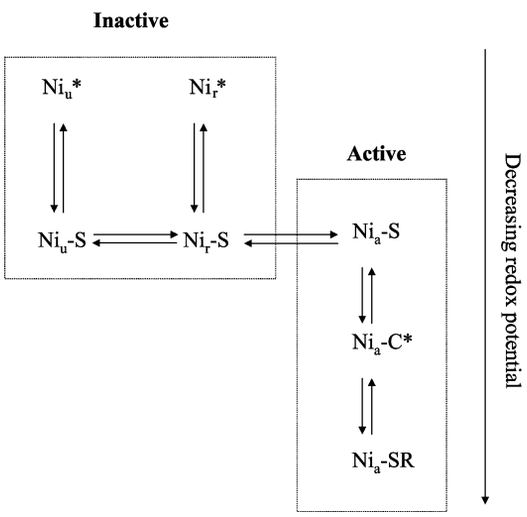

Scheme 1 Schematic representation of the spectroscopically characterized states of the [NiFe] active site of [NiFe]-hydrogenases. Notation is as follows: 'r' = 'Ready', 'u' = 'Unready' and 'a' = 'Active'. EPR-silent states are designated S, while EPR-detectable states are marked with a *. Vertical transitions correspond to one-electron redox reactions when measured in the presence of redox-mediating dyes. Alternative terminology has been used by different authors: the states may be translated as follows. Ni_u* = Ni–A; Ni_u–S = Ni–SI_u; Ni_r* = Ni–B; Ni_r–S = Ni–SI_r; Ni_a–S = Ni–SI_a; Ni_a–C* = Ni–C; Ni_a–SR = Ni–R.

The case of [NiFe]-hydrogenase highlights some interesting aspects of how properties of enzymes are revealed and how complexity is resolved using protein film voltammetry, simply because we use an electrode (specifically, a rotating disc electrode) to drive and measure reactions.[11,36] Furthermore, the entire enzyme sample under investigation (a minuscule quantity, of the order of a picomole or less) can be transferred on the electrode from one solvent to another, effecting an instantaneous "pico"-dialysis. A catalytic voltammogram provides a simple picture of how activity varies with potential. Fig. 2 shows some of the different shapes that are observed for voltammograms of [NiFe]-hydrogenase at different pH, temperature, and scan rate. To help follow the reasoning throughout this paper, we now explain, briefly, how these shapes arise.

For hydrogenase, the highest coverages we have achieved on an electrode surface are about 3×10^{-12} mol cm^{-2}. The high activity means that with even with this quite low coverage, oxidation of H_2 is usually diffusion controlled, and the limiting

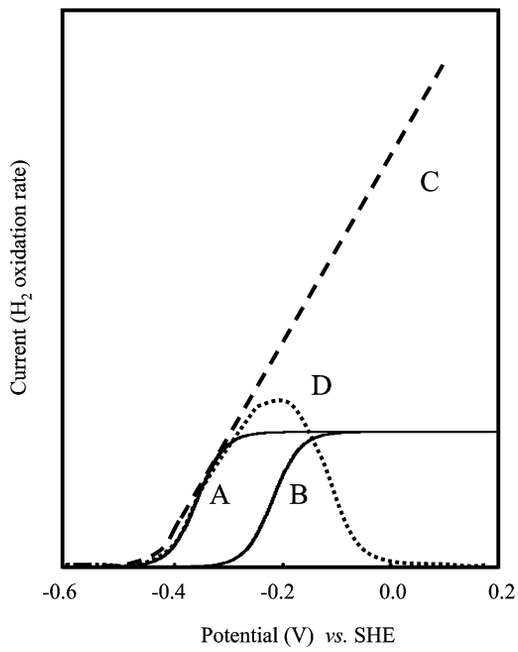

Fig. 2 Graphical representation showing the effect of different conditions on hydrogenase H_2 oxidation voltammetry. A: Fast scan rates (1 V s^{-1}), high pH (pH = 9) and *low temperatures* (10 °C). The cyclic voltammogram has a sigmoidal shape. B: Fast scan rates (1 V s^{-1}), low pH (pH = 5) and *low temperatures* (10 °C). The shape of the cyclic voltammogram is sigmoidal and the same limiting current is reached as at high pH, although the catalytic wave is now shifted to a more positive potential. C: Fast scan rate (1 V s^{-1}), high pH (pH = 9) and *high temperature* (45 °C). The cyclic voltammogram becomes steep and linear at high overpotential as interfacial electron transfer replaces inherent enzyme turnover as the rate determining factor. D: *Slow scan rates* (0.3 mV s^{-1}), high pH (pH = 9) and high temperatures (45 °C). At high potentials the catalytic current drops as the enzyme undergoes reversible anaerobic oxidative inactivation.

current obtained for 1 bar H_2 is the same as observed for a Pt electrode (*i.e.* about 4 mA cm^{-2} for a flat electrode at 45 °C).[7] All the voltammograms represented in Fig. 2 are summaries of real results and correspond to experiments in which the electrode is rotating at high speed and the enzyme coverage is low (after adsorbing to saturative coverage, the electrode surface is gently polished with a piece of cotton wool). First we consider situations A and B, which are each obtained for a film of hydrogenase at low temperature, at pH 9 and pH 5 respectively.[9] Clearly, the limiting current achieved at either pH is approximately the same (*i.e.* the turnover number is independent of pH) and the only difference is the shift to higher potential as the solution becomes more acidic. This stresses the advantage of electrochemical control, in that the driving force can be varied up to a high enough value that it no longer influences the reaction, so that we achieve a measure of the *inherent* activity of the enzyme; in fact the limiting current reflects the rate-determining step during catalysis. If we compare H_2 oxidation activities at some intermediate potential, say −0.3 V, *i.e.* between the two traces A and B, we might conclude instead that the activity at pH 9 is much higher than pH 5: but this would not reflect *inherent* activity. Situation C is encountered when the temperature is raised, other conditions being as for A: clearly, the high-potential region now resembles an Ohmic resistor.[8] This occurs because the activation energy for enzyme turnover is higher than for interfacial electron transfer (enzyme to electrode), so that the latter is now rate determining. There is now a strong dependence on potential, furthermore the electron coupling between the active sites and the electrode varies among the population of adsorbed enzyme molecules, and is poor in many cases, the overall result being to produce a linear relationship between current and potential.[8] Situation D adds

yet another dimension, since when subjected to oxidising potentials the enzyme converts to the inactive 'ready' state (Ni_r*: see Scheme 1) in which a bridging O-atom has been incorporated between the Ni and the Fe. This reaction is complicated (see below) but occurs more rapidly at pH 9 and higher temperatures.[10]

In this paper, we describe three studies that demonstrate how the remarkable electrocatalytic activity of [NiFe]-hydrogenase is used to answer some subtle questions. A fuller understanding of the rate-determining steps, and of the mechanisms of reaction with O_2 and CO are important issues that need to be addressed if these enzymes are to be exploited in new technology. A particular consideration is the ability to probe activity directly as a function of potential and drive interfacial electron transfer at a sufficiently high rate that it is not rate-determining. We describe experiments to measure the following:

1. The isotope effect on the rate of catalytic oxidation of H_2 (D_2) at different temperatures and potentials.

2. The reaction of hydrogenase with O_2, producing mixtures of 'ready' and 'unready' inactive forms.

3. The reaction of hydrogenase with CO and the binding strength of this inhibitor as a function of potential (*i.e.* of the oxidation state of the active site).

Experimental

The [NiFe]-hydrogenase from *Allochromatium vinosum* (*Av*H_2ase) was prepared as described previously.[37] The pyrolytic graphite edge (PGE) rotating disc electrode (area 3 mm^2) was used in conjunction with an EG&G M636 electrode rotator. The all-glass electrochemical cell incorporated a three-electrode configuration, and was equipped with an 'o'-ring gasket that fitted snugly around the electrode rotator to seal the internal atmosphere of the cell from that of the glovebox (M. Braun: N_2 with O_2 < 2 ppm). This allowed fast and precise exchanges of different gases. A platinum wire was used as counter electrode, and a saturated calomel electrode (SCE) in a Luggin side-arm containing 0.1 M NaCl was used as reference. The reference potential was corrected with respect to the standard hydrogen electrode (SHE) by using $E_{SHE} = E_{SCE} + 242$ mV at 25 °C, and all values quoted are with respect to SHE. The main compartment was jacketted and thermostatted at the required experimental temperature, while the reference electrode side arm was well separated and maintained at 25 °C.

Voltammetry and chronoamperometry were performed with an Autolab PGSTAT10 or PGSTAT20 electrochemical analyzer (Eco Chemie, Utrecht, The Netherlands) controlled by GPES software (Eco Chemie) and equipped with a digital (staircase) scan generator and an electrochemical detection (ECD) module for increased sensitivity. In chronoamperometry experiments, the current was sampled every second following the potential step.

Experiments were performed using a mixed buffer system consisting of sodium acetate, MES (2-[*N*′-morpholino]ethane-sulfonic acid), HEPES (*N*′-[2-hydroxyethyl] piperazine-*N*′-[2-ethane-sulfonic acid]), TAPS (*N*′-tris[hydroxymethyl] methyl-3-amino-propane-sulfonic acid), and CHES (2-[*N*′-cyclohexyl-amino]ethane-sulfonic acid); all purchased from Sigma, with final concentrations of 15 mM in each component and containing 0.1 M NaCl as additional supporting electrolyte. All solutions were prepared with purified water (Millipore: 18 MΩ.cm) and titrated with NaOH or HCl to the desired pH at the experimental temperature. To stabilise the film of hydrogenase on the electrode, a co-adsorbate, polymyxin B sulfate (Sigma) was added from a stock solution (10–20 mg ml^{-1}) to give a final concentration of 200 μg ml^{-1}. The pH values of final solutions were always checked after the experiment at the temperature used for measurements. Gases used in the experiments were N_2 (BOC), H_2 (Air Products), CO (BOC), O_2 (Air Products) and D_2 (BOC).

Before each experiment, the PGE electrode was polished with an aqueous alumina slurry (Buehler, 1 μm) and sonicated thoroughly. To prepare a protein film, the stationary electrode was placed into a dilute solution of hydrogenase (0.1–1.0 μM, pH 7; 45 °C, containing polymyxin B sulfate) while cycling the electrode potential between −558 mV and +242 mV at 10 mV s^{-1} until a stable catalytic response was obtained, as described previously.[6,10] This typically requires 20 minutes, following which the electrode exhibits diffusion-controlled H_2 oxidation when H_2 is introduced to the cell. Since such high activity presents a problem for studies designed to measure small changes in enzyme activity (diffusion control masks details of the catalytic properties of the enzyme), the electrode was then re-polished with a piece of damp cotton wool to lower the enzyme coverage to such a level that the catalytic current obtained in the presence of H_2 was independent of electrode rotation rate above 1500 rpm (see below). The cell solution was then replaced with an enzyme-free solution (*ca.* 5 ml): this is important as it overcomes the problem of enzyme molecules on the electrode surface that have been held under strict potential control exchanging with 'free' enzyme molecules in solution, thereby corrupting the results.

Results and discussion

The H/D isotope effect on catalytic H_2 oxidation

Reports in the literature have suggested that while processes such as H_2/H_2O exchange are subject to a significant isotope effect, the rate of oxidation of H_2 is the same as for oxidation of D_2.[27,38] However, these experiments were carried out using conventional 'enzyme assay' methods – measuring the rate of reduction of dyes such as methyl viologen – and the turnover rates reported are much lower than we have observed using electrochemistry.[38] For example, a zero isotope effect has been argued on the basis of experiments in which the measured turnover number is just 27 s^{-1}! An obvious problem here is that the oxidant, methyl viologen, provides only a tiny driving force, well below that required to detect any inherent limiting factor within the enzyme.

Fig. 3A shows how the catalytic oxidation current for a hydrogenase film, measured at 10 °C, pH 6, rises and drops by a constant fraction as the headgas is switched repeatedly between 1 bar H_2 and 1 bar D_2. The potential is held at a positive value (242 mV) in the plateau region of the voltammogram (see traces A and B, Fig. 2), the object being to provide a high driving force to ensure that the rate relates as closely as possible to the limiting step of turnover. Over the period of the experiment, there is a slow underlying decrease in the amplitude, due mainly to oxidative transformation to the inactive 'ready' state, as well as some desorption of enzyme.

The experiment shows clearly that there is an isotope effect of 1.55: this is small, but significant compared to the reported value of 1.0, which suggested, incorrectly, that the rate-determining effect has nothing to do with the transport, binding or activation of H^+ or H_2. Fig. 3B shows the results of experiments carried out at the higher temperature of 45 °C, at which the rate-determining step is shifted towards interfacial electron transfer (see Fig. 2, trace C). The isotope effect is now much smaller, at just 1.15: this is reasonable, since electron transfer should be less sensitive to H/D substitution. There is also a more noticeable underlying decrease in activity, since conversion to the inactive 'ready' state of the enzyme (see Scheme 1) is faster at high temperature.[10] Finally, Fig. 4 shows how the H/D isotope effect depends on potential. The series of experiments carried out at 10 °C show that the isotope effect *decreases* as the potential is made more negative. Indeed, at −358 mV, which is close to the driving force provided by methyl viologen in the conventional solution experiments, the rates of oxidation of H_2 and D_2 are essentially the same.

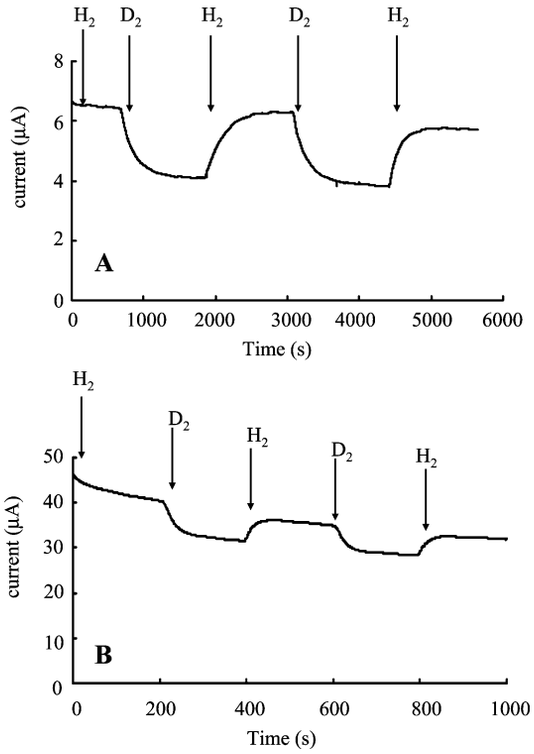

Fig. 3 (A) Chronoamperometry at 10 °C, 242 mV, pH 6.0, electrode rotation rate 2500 rpm. As the gas (1 bar) above the cell solution is interchanged between H_2 and D_2, a kinetic isotope effect of 1.55 is observed. (B) Chronoamperometry at 45 °C, 242 mV, pH 6.0 and electrode rotation rate 2500 rpm. As the gas above the cell solution is interchanged between H_2 and D_2, a kinetic isotope effect of 1.15 is observed.

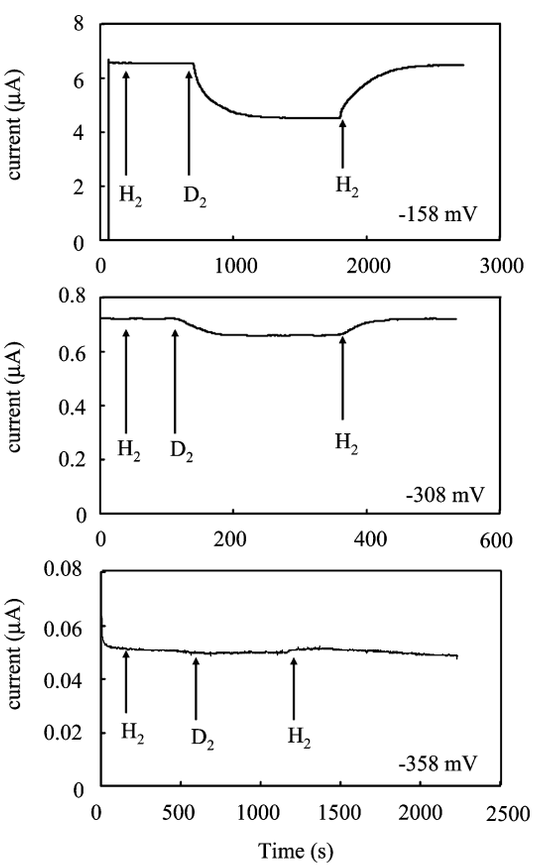

Fig. 4 Chronoamperometry at 10 °C, pH 6.0 and electrode rotation rate 2500 rpm, at the potentials indicated. As the gas in the cell above the solution is interchanged between H_2 and D_2, a kinetic isotope effect of 1.44 is observed at −158 mV, which drops to 1.1 at −308 mV and to 1.0 at −358 mV.

The reactions of hydrogenase with O_2

It has been reported that the reaction of [NiFe]-hydrogenases with O_2 produces mainly the 'unready' state, whereas anaerobic oxidation results in the 'ready' state.[19] Previous studies in this laboratory have shown that enzyme molecules that have been inactivated anaerobically, *i.e.* by applying a positive potential at the electrode, undergo a rapid and almost complete recovery as the potential is swept or stepped to a negative potential. This is fully consistent with activation of 'ready' rather than 'unready' enzyme.[10] The rate of activation increases as a more negative potential is applied, which is as expected if removal of the bridging O-ligand is preceded by rate-limiting reduction of Ni(III) to Ni(II). The behaviour pattern thus provides a convenient and quantifiable signature for formation of the 'ready' state, and we have extended the principle to study the reaction of hydrogenase with O_2 and compare the characteristics of aerobic *vs.* anaerobic inactivation.

Fig. 5A compares two chronoamperometry experiments, in which the H_2 oxidation rate is monitored as a function of time, at 45 °C, while applying a high potential, *i.e.* 242 mV. At pH 6, oxidative inactivation is slow; but injection of O_2-saturated buffer causes rapid and complete loss of activity. Fig. 5B shows a voltammogram measured at a very slow scan rate, during the course of which O_2-saturated buffer is injected. As expected, the activity vanishes immediately, but as the cycle continues, O_2 is swept from the solution and headspace by flushing with H_2, and the enzyme reactivates as the potential drops below −100 mV. This potential is similar to that measured for reactivation after *anaerobic* inactivation, suggesting that the same species is formed regardless of the oxidising agent. However not all the enzyme is reactivated in this fast process, and to probe this further we designed a more detailed experiment that uses a potential-step sequence. This is shown in Fig. 6.

Initially, the H_2 oxidation activity is followed for a period of time at a potential of −88 mV, then O_2 is injected and the current drops immediately to zero. The potential is then stepped to 242 mV, while the solution and headspace are purged with H_2

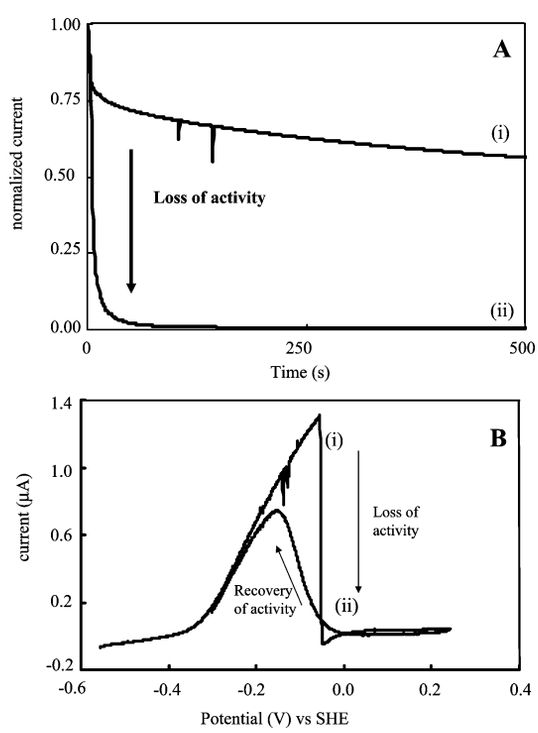

Fig. 5 (A) Chronoamperometry at 242 mV, 45 °C, pH 6.0 and electrode rotation rate 2500 rpm. Trace (i) shows anaerobic oxidative inactivation (slow), (ii) shows aerobic inactivation (fast). (B) Cyclic voltammetry at slow scan rate (1.2 mV s^{-1}), pH 6.0, 45 °C and electrode rotation rate 2500 rpm. O_2-saturated buffer is injected into the cell solution at (i) and then flushed out by passing H_2 into the cell at (ii).

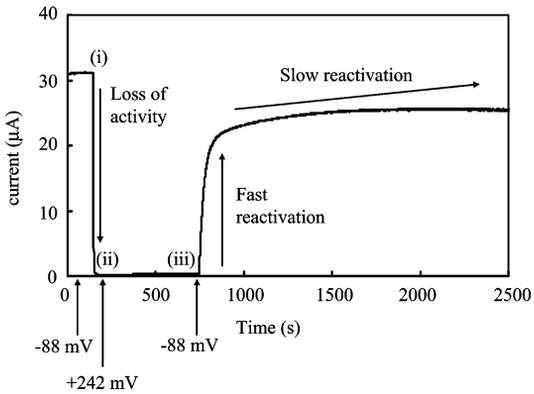

Fig. 6 Chronoamperometry at −88 mV, pH 6.0, 45 °C and electrode rotation rate 2500 rpm. At (i) 250 μl of O_2 saturated buffer is injected into the cell causing rapid loss of activity. At (ii) the potential is then raised to 242 mV (to prevent reactivation of the enzyme while O_2 is still present in the cell) and the cell is flushed with H_2 to remove any traces of O_2 from solution. At (iii) the potential is then stepped back to −88 mV to induce reactivation.

to remove O_2. Then the potential is stepped back to −88 mV to observe reactivation. This occurs in *two* stages: the first stage is fast, consistent with activation of the 'ready' state. This is followed by a slow phase, occurring over the course of about half an hour and accounting for about 20% of the total amplitude.

These results show that O_2 produces two different inactive forms that can be activated by reduction: one of these is re-activated much more rapidly than the other, with rates similar to those measured previously for the anaerobically inactivated form assigned as 'ready'.[10] Formation of 'ready' by the aerobic route is much faster than achieved by anaerobic reaction – likely reasons being that O_2 reacts *via* an inner-sphere mechanism, or that unlike the anaerobic route, both electron removal and ligand incorporation are achieved with a single attacking entity.

The reaction of enzyme with CO

Carbon monoxide is a competitive inhibitor of hydrogenase, and the reaction is readily reversible, unlike the reaction with Pt. We have examined the rates of recovery of [NiFe]-hydrogenase after complete inhibition with CO, as a function of potential, in order to establish if we could bias the system in any way to reveal oxidation states to which CO is much more tightly bound (see Scheme 1). The results are shown in Fig. 7.

In Fig. 7A, CO is introduced into the cell, then as it is swept out of the headspace by H_2, activity is recovered. Fig. 7B shows that the rate of recovery does not depend on the potential that is applied. This suggests strongly that recovery depends only on the rate of physical gas exchange between headspace and solution. Release of CO from the active site must be relatively fast, and it is not possible to isolate, by imposing the appropriate potential, any particular oxidation state that is able to bind CO more tenaciously.

Conclusions

These results demonstrate how the activity of a complex enzyme can be monitored and controlled under conditions that are far more precise than can normally be achieved in conventional homogeneous experiments. The H_2/D_2 isotope effect measurements and CO recovery experiments are already quite definitive, while the studies with O_2 serve to stress the complexity of these transformations. The drawback with these studies is that no structural information is obtained, so that correlations with spectroscopically-defined states rely on similarities in formation conditions and kinetics. Despite this aspect, direct electrochemical experiments on minuscule samples of hydrogenase are yielding new kinetic data, with high precision and sensitivity, in the 'potential dimension'.

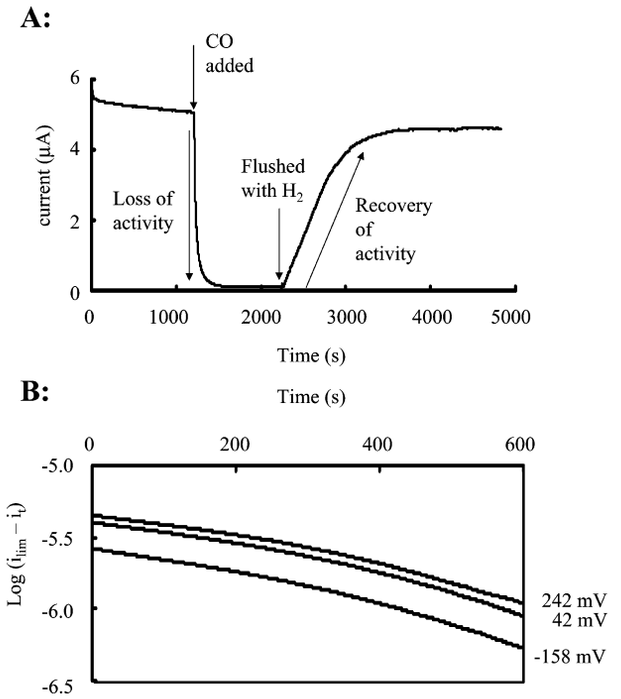

Fig. 7 (A) Chronoamperometry experiments at 242 mV, pH 6.0, 25 °C and electrode rotation rate 2500 rpm. Addition of CO to the headspace results in a decrease in current. When CO is subsequently flushed out of the headspace by H_2, the activity returns. (B) Semi-log plots of $\log(i_{lim} - i_t)$ *vs.* time (where i_{lim} = limiting catalytic current at high potential after removal of CO and i_t = the current at time t) showing the recovery of activity after removal of CO for the data shown in *A* (242 mV). Data for analogous experiments performed at the potentials indicated are also shown.

Appendix

The activity of an enzyme adsorbed on an electrode is quantified by an expression (A1)

$$\frac{1}{i_{lim}} = \frac{(C + K_M)}{nFA\Gamma k_{cat} C} + \frac{1}{0.62\, nFAD^{2/3} C\, \nu^{-1/6} \omega^{1/2}} \qquad \text{(A1)}$$

that is derived by combining the Michaelis–Menten equation, which relates the catalytic current to substrate concentration C and Michaelis constant K_M, with the Levich equation, which relates the current to the rotation rate of the electrode ω.[39] In eqn. (A1) the limiting current i_{lim} is the value observed at the plateau of sigmoidal-type catalytic voltammograms as represented by 'A' and 'B' in Fig. 2A. The form of this wave shows the importance of the ability to vary potential to obtain an optimum rate. Other terms are as follows: n is the stoichiometric number of electrons used in the reaction (2.0 for oxidation of H_2), F is the faraday constant, Γ is the electroactive coverage of enzyme on the electrode surface, D is the diffusion coefficient of the substrate, and ν is the kinematic viscosity of the solvent (water). For hydrogenase, a value or lower estimate for Γ is obtained from the size of the faint peak-type signal, assigned to reversible electron transfers with the $[3Fe\text{-}4S]^{+/0}$ cluster, that can be observed under non-catalytic conditions (N_2 atmosphere or CO-inhibited).[6]

Readily visualised limiting cases occur first (A2) when ω is large (this is obtained from intercepts of the plots of $1/i_{lim}$ against $1/\omega^{-1/2}$) so that the second term vanishes

$$\frac{1}{i_{lim}} = \frac{(C + K_M)}{nFA\Gamma k_{cat} C} \qquad \text{(A2)}$$

then when $C \gg K_M$ (the enzyme is saturated with substrate) thus giving

$$i_{lim} = nFA\Gamma k_{cat} \quad \text{(A3)}$$

The turnover number is then simply given by

$$k_{cat} = \frac{i_{lim}}{nFA\Gamma} \quad \text{(A4)}$$

Acknowledgements

This research is supported by the EPSRC and BBSRC (43/E16711) and the Netherlands Organization for Scientific Research (NWO) division for Chemical Science. We thank Drs Harsh Pershad and Anne Jones for carrying out some of the earlier studies leading to the experiments we have described.

References

1 G. F. Bickerstaff, in *Molecular Biology and Biotechnology*, Royal Society of Chemistry, Cambridge, 4th edn., 2000, pp. 433–460.
2 G. C. Bond, *Heterogeneous Catalysis: Principles and Applications,* Clarendon Press, Oxford, 2nd edn., 1990.
3 A. M. Bond, *Broadening Electrochemical Horizons*, Oxford University Press, Oxford, 2002.
4 F. A. Armstrong, *J. Chem. Soc., Dalton Trans.*, 2002, **5**, 661.
5 A. A. Karyakin and S. D. Varfolomeev, *Russ. Chem. Rev.*, 1986, **55**, 867.
6 H. R. Pershad, J. L. C. Duff, H. A. Heering, E. C. Duin, S. P. J. Albracht and F. A. Armstrong, *Biochemistry*, 1999, **38**, 8992.
7 A. K. Jones, E. Sillery, S. P. J. Albracht and F. A. Armstrong, *Chem. Commun.*, 2002, 866.
8 C. Léger, A. K. Jones, S. P. J. Albracht and F. A. Armstrong, *J. Phys. Chem. B.*, 2002, **106**, 13058.
9 C. Léger, A. K. Jones, W. Roseboom, S. P. J. Albracht and F. A. Armstrong, *Biochemistry*, 2002, **41**, 15736.
10 A. K. Jones, S. E. Lamle, H. R. Pershad, K. A. Vincent, S. P. J. Albracht and F. A. Armstrong, *J. Am. Chem. Soc.*, 2003, **125**, 8505.
11 C. Léger, S. J. Elliott, K. J. Hoke, L. J. C. Jeuken, A. K. Jones and F. A. Armstrong, *Biochemistry*, 2003, **42**, in press.
12 *Hydrogen as a Fuel: Learning from Nature*, eds. R. Cammack, M. Frey and R. Robson, Taylor and Francis, London and New York, 2001.
13 P. M. Vignais, B. Billoud and J. Meyer, *FEMS Microbiol. Rev.*, 2001, **25**, 455.
14 S. P. J. Albracht, *Biochim. Biophys. Acta*, 1994, **1188**, 167.
15 S. P. J. Albracht, in *Hydrogen as a Fuel: Learning from Nature*, eds. R. Cammack, M. Frey, R. Robson, Taylor and Francis, London and New York, 2001.
16 A. Volbeda, M.-H. Charon, C. Piras, E. C. Hatchikian, M. Frey and J. C. Fontecilla-Camps, *Nature (London)*, 1995, **373**, 580.
17 A. Volbeda, E. Garcin, C. Piras, A. L. De Lacey, V. M. Fernandez, E. C. Hatchikian, M. Frey and J. C. Fontecilla-Camps, *J. Am. Chem. Soc*, 1996, **118**, 12989.
18 R. Happe, W. Roseboom, A. J. Pierik, S. P. J. Albracht and K. A. Bagley, *Nature (London)*, 1997, **385**, 126.
19 A. L. De Lacey, E. C. Hatchikian, A. Volbeda, M. Frey, J. C. Fontecilla-Camps and V. M. Fernandez, *J. Am. Chem. Soc.*, 1997, **119**, 7181.
20 K. A. Bagley, E. C. Duin, W. Roseboom, S. P. J. Albracht and W. H. Woodruff, *Biochemistry*, 1995, **34**, 5527.
21 K. A. Bagley, C. J. van Garderen, M. Chen, E. C. Duin, S. P. J. Albracht and W. H. Woodruff, *Biochemistry*, 1994, **33**, 9229.
22 J. C. Fontecilla-Camps, A. Volbeda and M. Frey, *Trends Biotechnol.*, 1996, **14**, 417.
23 J. P. Collman, *Nature Struct. Biol.*, 1996, **3**, 213.
24 M. J. Maroney and P. A. Bryngelson, *J. Biol. Inorg. Chem.*, 2001, **6**, 453.
25 P. E. M. Siegbahn, M. R. A. Blomberg, M. Wirstam and R. H. Crabtree, *J. Biol. Inorg. Chem.*, 2001, **6**, 460.
26 H.-J. Fan and M. B. Hall, *J. Biol. Inorg. Chem.*, 2001, **6**, 467.
27 P. Bertrand, F. Dole, M. Asso and B. Guigliarelli, *J. Biol. Inorg. Chem.*, 2000, **5**, 682.
28 A. L. De Lacey, V. M. Fernandez, M. Rousset, C. Cavazza and E. C. Hatchikian, *J. Inorg. Biol. Chem.*, 2003, **8**, 129.
29 D. P. Barondeau, L. M. Roberts and P. A. Lindahl, *J. Am. Chem. Soc.*, 1994, **116**, 3442.
30 L. M. Roberts and P. A. Lindahl, *J. Am. Chem. Soc.*, 1995, **117**, 2565.
31 A. Volbeda, Y. Montet, X. Vernède, E. C. Hatchikian and J. C. Fontecilla-Camps, *Int. J. Hydrogen Energy*, 2002, **27**, 1449.
32 C. Stadler, A. L. de Lacey, Y. Montet, A. Volbeda, J. C. Fontecilla-Camps, J. C. Conesa and V. M. Fernandez, *Inorg. Chem.*, 2002, **41**, 4424.
33 M. Carepo, D. L. Tierney, C. D. Brondino, T. C. Yang, A. Pamplona, J. Telser, I. Moura, J. J. G. Moura and B. M. Hoffman, *J. Am. Chem. Soc.*, 2002, **124**, 281.
34 R. R. Happe, W. Roseboom and S. P. J. Albracht, *Eur. J. Biochem.*, 1999, **259**, 602.
35 B. Bleijlevens, B. W. Faber and S. P. J. Albracht, *J. Biol. Inorg. Chem.*, 2001, **6**, 763.
36 H. A. Heering, J. Hirst and F. A. Armstrong, *J. Phys. Chem. B.*, 1998, **102**, 6889.
37 J. M. C. C. Coremans, J. W. van der Zwaan and S. P. J. Albracht, *Biochim. Biophys. Acta*, 1992, **1119**, 157.
38 N. A. Zorin, B. Dimon, J. Gagnon, J. Gaillard, P. Carrier and P. M. Vignais, *Eur. J. Biochem.*, 1996, **241**, 675.
39 A. Sucheta, R. Cammack, J. Weiner and F. A. Armstrong, *Biochemistry*, 1993, **32**, 5455.